Proceedings of the Combustion Institute 41 (2025) 105858

Contents lists available at ScienceDirect

Proceedings of the Combustion Institute

journal homepage: www.elsevier.com/locate/proci

Effect of H_2 and Jet-A1 fuel split on flame stability and pollutant emissions from low-swirl burner

Samarjeet Singh [a,*], Matteo Amerighi [b], Nicola Scopolini [b], Antonio Andreini [b], Stefan R. Harth [a], Dimosthenis Trimis [a]

[a] Engler-Bunte-Institute, Division of Combustion Technology, Karlsruhe Institute of Technology, Karlsruhe, 76131, Germany
[b] Department of Industrial Engineering, University of Florence, Florence, 50139, Italy

ARTICLE INFO

Keywords:
Dual-fuel combustion
Hydrogen combustion
Flame lift-off
Jet in cross-flow
Fuel-flexible combustor

ABSTRACT

Hydrogen combustion is emerging as a promising solution for future aircraft engines, offering a shift from fossil fuels to sustainable alternatives and the potential for reduced pollutant emissions. While the complete transition to H_2 presents a significant challenge due to its low volumetric energy density, limited availability, and infrastructure and aircraft redesign constraints, fuel-flexible burner technologies that allow H_2 blending with Jet-A1 offer a viable alternative. These technologies provide additional benefits such as an enhanced stability range and can contribute to achieving near-term decarbonization goals. This study explores the capabilities of a novel dual-fuel burner developed as part of the European project FFLECS (Novel Fuel-Flexible ultra-Low Emissions Combustion systems for Sustainable aviation). Flame stabilization in a lean lifted flame combustor operating under atmospheric conditions and fueled by Jet-A1 and H_2 is experimentally investigated. A new fuel-flexible nozzle, based on the "low swirl" lean lifted flame concept, is developed to enable high premixing, significantly reducing NO_x emissions and minimizing flashback risk compared to conventional swirl-stabilized flames. The H_2 injection for the investigated nozzle was optimized for part load conditions, but can still be operated up to 100% H_2. The flame shape and lift-off height were studied at elevated air inlet temperature and H_2 blending ratios up to 100% of the total thermal power. Moreover, the lean blowout limits remain similar for H_2 blending ratios up to 30% across various air inlet temperatures but change significantly at higher blends. Finally, switching from Jet-A1 to H_2 lowers NO_x emission at low air inlet temperatures and increases it at higher temperatures, with a pronounced rise across all air inlet temperatures at blends above 75% H_2 under elevated specific thermal power. In contrast, the NO_x emissions remain consistently very low at low specific power close to the lean blowout limit. Additionally, even a modest H_2 fuel split of 15% significantly reduces CO emissions. These findings highlight the potential of H_2 addition to lean lifted spray flame utilizing Jet-A1, facilitating the future development and optimization of fuel-flexible combustors for aircraft engines.

1. Introduction

Hydrogen (H_2) has emerged as a promising candidate for future air transportation, attracting attention for its high energy density per unit mass and its ability to produce zero carbon emissions [1]. Nevertheless, the adoption of H_2 as an aviation fuel has faced significant limitations, primarily due to its low volumetric energy density, storage and handling challenges, infrastructure constraints, and the need for major aircraft design modifications depending on flight range. These challenges make it unlikely that H_2 will see widespread use in aviation before the end of this decade [2–4].

Fuel-flexible systems provide a practical route to integrate H_2 into aviation without full aircraft redesign [5]. These systems, utilizing conventional fuels with limited H_2 injection, can reduce local pollutant emissions near airports and lower overall CO_2 across the flights, without restricting flight range. Their ability to operate on both H_2 and conventional fuel makes them an attractive approach for faster deployment. However, due to the differences in the physical properties of H_2-rich fuel mixtures compared to aviation fuel, well-established combustion systems cannot be directly applied for low NO_x and stable combustion. The increased fuel reactivity and higher flame speed of H_2 can significantly alter flame anchoring position and, in extreme cases, lead to flashback [6]. Hence, designing a flashback-proof and low emissions combustor for dual fuel mixture remains a significant challenge.

* Corresponding author.
E-mail address: samarjeet.singh@kit.edu (S. Singh).

https://doi.org/10.1016/j.proci.2025.105858
Received 2 May 2025; Accepted 4 September 2025
Available online 24 September 2025

To prevent flashback and maintain low emissions, innovative fuel nozzle designs, such as micro-mix, have been proposed by Funke et al. [7], where the fuel gets injected in jet in cross-flow configuration into the air through small air guiding panel structures. The fuel injection through multiple miniaturized fuel jets results in the formation of micro flames, producing low NO_x emissions and providing inherent safety against flashback. By employing a micro-mixing fuel injection strategy for H_2, rapid mixing is achieved alongside the inherent flexibility needed to support various staging, dilution, and dual-fuel configurations in next-generation gas turbine engines [8]. Moreover, the high diffusivity of H_2 jet is expected to have a substantial impact on the mixing process [9]. Chen et al. [10] compared swirl and non-swirl micromix combustors, showing that swirl nozzles offer better mixing uniformity, higher lean blow-off limits, and lower NO emissions than non-swirl nozzles.

However, more complex architectures involving non-swirled cross-flow injections interacting with swirling flows have recently been investigated [11] as a potential strategy to stabilize H_2 flames in modern gas turbines. To accommodate H_2-rich combustion, recent designs further enhance flashback safety by incorporating the non-swirling airflow along the central axis of the radial swirl generator [12]. Building on these efforts, Reichel et al. [13] applied axial air injection to create a plug-flow like velocity profile at the nozzle exit to eliminate flashback in a H_2 fueled swirl-stabilized combustor.

Several experimental [14–19] and theoretical [20–22] investigations have contributed significantly towards the dual fuel operation of H_2 and conventional aviation fuels. Notably, Hiroyasu et al. [14] conducted the pioneering experimental study covering the full range of H_2–kerosene blends (0–100% H_2). Their work demonstrated how variations in H_2 concentration influence flame stability, combustion efficiency, and pollutant emissions. Similarly, other studies [15–18], albeit utilizing lower H_2 blending ratios, have highlighted changes in the flammability limits, flame structure, and pollutant emission formation. More recently, Dave et al. [19] presented a unique combustor capable of operating with 0 to 100% H_2 fuel split, featuring a centrally located premixed swirl-stabilized H_2 flame flanked by kerosene flames. They observed strong acoustic tonal behavior in pure H_2 or pure kerosene modes. However, to the best knowledge of the authors, no previous studies have explicitly addressed the challenges in achieving stable combustion ranging from pure aviation fuel to pure H_2 through intermediate blends. Moreover, dual-fuel experiments under engine-relevant conditions are critical for advancing next-generation engine development.

In this study, the influence of elevated air inlet temperature (T_{air}) on flame shapes, lean blowout limits (LBO), and pollutant emissions in the fuel-flexible combustor operating under atmospheric conditions is investigated. The burner employs Jet-A1 fuel via an atomizer, alongside H_2 injected in a jet in cross-flow configuration. Our work uniquely explores dual-fuel combustion by integrating H_2 with a lean-lifted spray Jet-A1 flame. It is analyzed how the flame shape changes with increasing H_2 concentration at various T_{air}. Most importantly, the lift-off heights (LOH) and LBO limits across different fuel mixtures are compared and safety margins for flame flashback are determined. Finally, the NO_x and CO emissions at elevated T_{air} with varying H_2 content and two specific thermal powers are analyzed.

2. Experimental setup and measurements

2.1. Combustion facility and operating conditions

Experiments were performed on a laboratory-scale fuel-flexible combustor, which aims to achieve low NO_x emissions when burning H_2 and Jet-A1 fuels. The snapshot of the combustor is shown in Fig. 1(a). The setup consists of an air supply plenum, a combustion chamber with optical access, and an exhaust. The incoming air from the compressor is preheated up to 670 K with electrical heaters and fed to the air supply

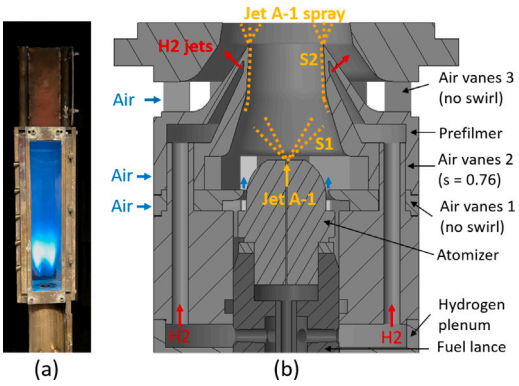

Fig. 1. (a) Photograph of a lab-scale gas turbine combustion chamber facility at Karlsruhe Institute of Technology (KIT) and (b) Schematic of the nozzle cross-section used for the investigation.

plenum, which includes a flow straightener. The combustor has a cross-sectional area of 100 × 100 mm^2 and a height of 460 mm, measured from the burner exit. This chamber is enclosed by quartz glass on all sides to facilitate optical access for detailed measurements. The exhaust section is open to the ambient environment, allowing the burned gases to exit into an extraction unit.

Fig. 1(b) shows the schematic of the investigated burner. The nozzle for dual-fuel operation is based on the one used by Shamma et al. [23], a nozzle developed for Jet-A1 only operation. The current nozzle includes two main air supplies (Air vanes 2 and 3) separated by a prefilmer lip. Only the Air vanes 2 impose a swirl on the flow. An additional small non-swirled airflow is entering by the Air vanes 1 to prevent flame flashback near to the nozzle axis. Both Jet-A1 and H_2 are supplied to the nozzle from the bottom of the burner via a fuel lance as shown in Fig. 1(b). The fuel lance is water-cooled to maintain the fuels at room temperature, preventing coking of the Jet-A1. Jet-A1 fuel is injected via a hollow cone atomizer mounted axially in the burner, characterized by a flow number of 0.74, a bore diameter of 0.35 mm, and a nominal spray inner half-angle of 60°. An airblast atomization system is employed, wherein the fuel atomization occurs in two consecutive steps (S1 and S2), as illustrated in Fig. 1(b). In the first step, the fuel is injected by a pressure atomizer (S1), forming a liquid film on the prefilmer. In the second step (S2), this film is atomized within the shear layers generated between the two air streams at the prefilmer tip. The H_2 is injected through 12 holes of 0.35 mm diameter at the outer prefilmer on an annular ring into the air crossflow from the Air vanes 3. The Air vanes 1 consists of eight straight vanes and the Air vanes 3 has twelve straight vanes, both with zero trailing angle and zero swirl number. The Air vanes 2 consists of eight tangentially inclined vanes and the vane trailing-edges are at an angle of 45 ° relative to the injector axis. The burner exhibits a relatively low overall swirl number around 0.1 (no inner recirculation zone targeted), calculated from the axial and angular momentum contributions of the three Air vanes and normalized by the burner exit radius [24].

Jet-A1 fuel mass flow rate was measured by Coriolis mass flow meters (Krohne OPTIMASS 3400c), with an accuracy of 0.1% of the measured value and a maximum flow capacity of 4.72 g/s. H_2 fuel mass flow rates are measured by a thermal mass flow controller (Bronkhorst EL-Flow) with an accuracy of 0.1% of full scale output and an operating capacity up to 0.68 g/s. The total airflow rate is measured by a thermal flow meter (Bronkhorst In-Flow) with an accuracy of 0.5% of full scale output and a maximum flow capacity of 348 g/s. The operating conditions of the experimental campaign at different arrangements are illustrated in Table 1.

When blending H_2 with Jet-A1 under constant thermal power (P) and fixed air mass flow rate ($\dot{m}_{air}$), the H_2 fraction in the dual-fuel mixture is defined as: $\%H_2 = \dot{m}_{H_2} Q_{H_2} / (\dot{m}_{H_2} Q_{H_2} + \dot{m}_{Jet\text{-}A1} Q_{Jet\text{-}A1})$ [14],

Table 1
Operating conditions of the fuel-flexible combustor considered in this study.

OC #	T_{air} (K)	$\dot{m}_{Jet\text{-}A1}$ (g/s)	$\dot{m}_{H_2}$ (g/s)	$\dot{m}_{air}$ (g/s)	$\mathcal{P}$ (kW)	$\mathcal{P}_{sp}$ (MJ/kg$_{air}$)	Δp/P(%)	U_b (m/s)
1	473	0–0.86	0–0.31	25.3	37.1	1.46	3	75.8
2	573	0–0.78	0–0.28	23	33.8	1.46	3	83.5
3	673	0–0.72	0–0.26	21.2	31.1	1.46	3	90.5
4	573	0–0.55	0–0.20	23	23.6	1.02	3	83.5

where Q denotes the lower heating value, with $Q_{H_2} = 119.97$ MJ/kg and $Q_{Jet\text{-}A1} = 43.1$ MJ/kg. Here, $\dot{m}_{H_2}$ and $\dot{m}_{Jet\text{-}A1}$ denotes the mass flow rate of H_2 and Jet-A1, respectively. For fuel-flexible combustion, the equivalence ratio (ϕ) is determined as: $\phi = [\dot{m}_{Jet\text{-}A1}/\dot{m}_{air} \cdot (1+\alpha)]/F^{\circ}_{Blend}$, where $\alpha = \dot{m}_{H_2}/\dot{m}_{Jet\text{-}A1}$ and the stoichiometric fuel–air ratio of the blend, F°_{Blend}, is given by: $F^{\circ}_{Blend} = (1+\alpha)/\,(1/F^{\circ}_{Jet\text{-}A1} + \alpha/F^{\circ}_{H_2})$ [16].

2.2. Measurement techniques

The side-view OH* chemiluminescence images of the flame are captured using a high-speed camera (Phantom V1212) coupled with a high-speed intensifier (LaVision HS-IRO). A 100 mm f/2.8 UV lens (Cerco) is used along with bandpass filters centered around OH* (Chroma, $T > 80\%$ in the spectral range between 300 − 340 nm, FWHM 10 nm). The camera was operated at a sampling frequency of 1 kHz for a total measurement time of 10 s and a pixel resolution of 1280 × 800.

For exhaust gas measurements, an active heated probe with a 6 mm inner diameter is located 440 mm downstream of the fuel nozzle. The gas sample is directed through a gas dehydrator to each analyzing module under controlled pressure conditions. Advanced Optima exhaust gas analysis system determines the concentration of O_2 (ABB Magnos 206), and the concentrations of CO and CO_2 (ABB Uras 26). For the determination of NO_x (i.e., NO and NO_2), an Eco Physics CLD 700 EL is used. Emission data for each H_2 content were acquired for 30 s at 1 Hz after reaching steady state.

3. Nozzle concept design

The major design considerations and working principles of the newly developed fuel-flexible nozzle are explained based on numerical simulations of the flow and mixing field. A preliminary non-reactive RANS simulation is performed for H_2 fuel only, with $\dot{m}_{H_2}$ set to 30% of the maximum value specified under operating condition 3 in Table 1. The simulation is carried out with the commercial pressure-based CFD solver ANSYS Fluent 23R2 and the k-ω model is adopted for the turbulence modeling, imposing a constant Schmidt and Prandtl number of 0.5. Moreover, a mixture-averaged approach is adopted to account for the fast diffusion of H_2 in the mixing process.

Fig. 2 shows the axial velocity distribution within the nozzle and combustion chamber. Of major importance for flame stabilization is the region near the outer recirculation zone, which is depicted by a graphical representation. A large lift-off height can be achieved by minimizing or completely avoiding fuel in the marked region (shown in white) of low/moderate air velocities in Fig. 2. The lift-off height is then mainly governed by the mixing process of the hot recirculated exhaust gases with fresh air and fuel. This principle is important as it enables a suitable design for the largely different burning velocities of Jet-A1 and H_2.

In this configuration of the nozzle, the H_2 is introduced by 12 H_2 jets at the outer sides of the prefilmer. The optimal H_2 jet in cross-flow penetration is designed for up to 30% of H_2 and a momentum flux ratio $J \leq 7.2$ to avoid burnable mixture near to the wall of the nozzle at the burner exit, thus avoiding a stabilization of the flame directly at the nozzle exit and enabling a higher lift-off height and related premixing. The momentum flux ratio is defined as the ratio between the hydrogen jet and free-stream air momentum fluxes: $J = \rho_{H_2} u^2_{H_2} / \rho_{air} u^2_{air}$, where ρ and u denote the density and velocity of the respective flows. Most importantly, a large radial jet penetration may

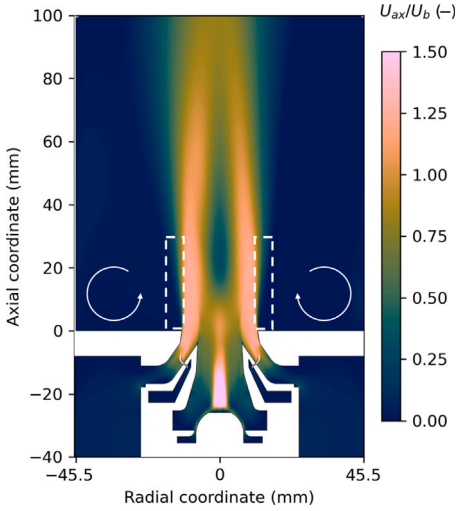

Fig. 2. RANS axial velocity field and schematic of the flame stabilization mechanism in the fuel-flexible nozzle.

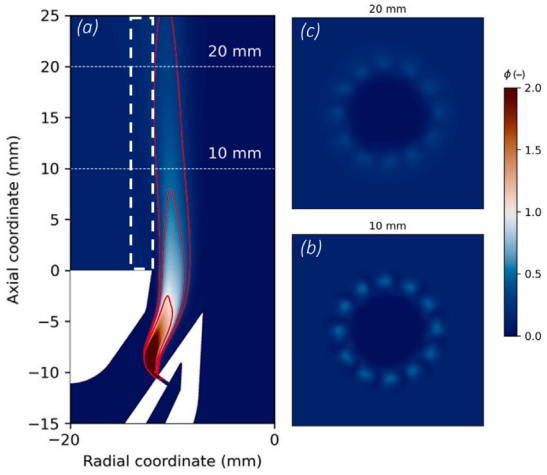

Fig. 3. RANS H_2 equivalence ratio (ϕ) distribution: (a) mid-plane and cross-sectional views at (b) 10 mm and (c) 20 mm above the nozzle exit.

enhance the lean blowout limits, as the outer recirculation zones in the combustor are essential for the stabilization of such flames. This improvement, however, comes with the drawback of increased NO_x emissions under part-load conditions. Therefore, using an increased number of H_2 injection holes when operating with higher H_2 content, could be advantageous in reducing NO_x emissions.

The mixing characteristics of air and fuel before combustion play a crucial role in flame stabilization and pollutant emission formation. Fig. 3 illustrates the H_2 equivalence ratio (ϕ) distribution on the mid-plane and at two cross-sections, located 10 mm and 20 mm downstream of the nozzle. The downstream spatial locations of $\phi = 1$, 0.5, 0.25 are indicated by three red isolines, which are superimposed on the mid-plane view, as shown in Fig. 3(a). No burnable mixture reaches the outer injector wall, proving the flashback safe design for these

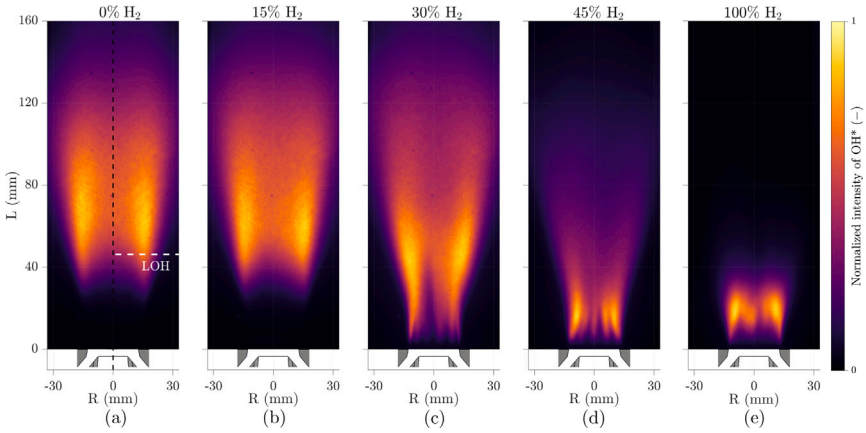

Fig. 4. Time-averaged OH* chemiluminescence images of flame for different H_2 and Jet-A1 fuel splits at air preheating temperature of T_{air} = 473 K, with constant $\dot{m}_{air}$ (corresponding to $\Delta p/P$ = 3%) and specific thermal power of $\mathcal{P}_{sp,1}$ = 1.46 MJ/kg$_{air}$. The equivalence ratios for the fuel splits are ϕ = 0.50, 0.49, 0.48, 0.47, and 0.42 for cases (a)–(e), respectively.

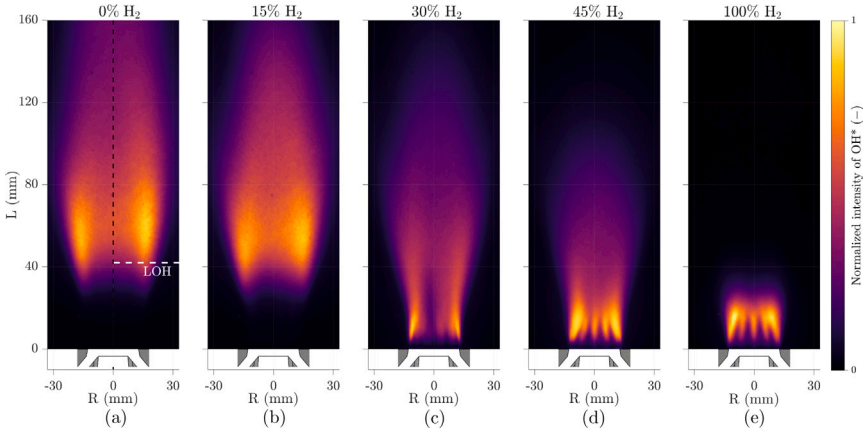

Fig. 5. Time-averaged OH* chemiluminescence images of flame for different H_2 and Jet-A1 fuel splits at T_{air} = 673 K, with constant $\dot{m}_{air}$ (corresponding to $\Delta p/P$ = 3%) and $\mathcal{P}_{sp,1}$ = 1.46 MJ/kg$_{air}$. Equivalence ratios are identical to those shown in Fig. 4.

operating conditions with 30% H_2 content. The fast mixing achieved by the jet in cross-flow injection strategy is further supported by the limited axial extension of the stoichiometric isoline, which does not reach the burner exit. Despite a certain level of unmixedness still present at 10 mm plane (Fig. 3b), only mixtures with $\phi < 0.5$ are present at this axial location. Finally, further downstream (Fig. 3c) a leaner and more uniform equivalence ratio distribution is observed.

Several additional measures were implemented to further minimize the risk of flame flashback and increase the lift-off height for operation with higher H_2 content. This design modification, compared to Shamma et al. [23], intended for Jet-A1 only operation, effectively eliminates the diffuser at the burner exit, ensuring a more streamlined airflow as shown in Fig. 2. In addition, turbulence generation within the Air vanes 3 (Fig. 1) was minimized by designing smooth area changes between vanes, preventing excessively high turbulent burning velocities and eliminating low air velocity zones in the mixing section of the nozzle. This change is important for mitigating the risk of flame flashback. Another feature of the nozzle is that the H_2 injectors are mounted perpendicular to the airflow, but are tilted at 55° relative to the nozzle axis. As a result, higher H_2 content increases the axial velocity component and improves the flashback limit. To further decrease the flashback propensity, an additional non-swirled air inlet was introduced near the nozzle axis around the atomizer as shown in Fig. 2. This axial jet decreases the velocity deficit on the center line of the swirling flow and shifts the region of lower axial velocity downstream within the combustor.

4. Experimental results and discussions

First, the morphological transitions of flame based on OH* chemiluminescence operating from 0 to 100% H_2 are discussed. Following this, the LOH and LBO across three different T_{air} are analyzed. Finally, the combustor performance is evaluated under different operating conditions by analyzing the measured NO_x and CO emissions.

4.1. Flame shape during fuel-flexible operation

Fig. 4 shows the time-averaged OH* chemiluminescence images of the different flame shapes observed in the experiments for fuel blends with H_2 splits ranging from 0 to 100% at T_{air} = 473 K, thermal power of $\mathcal{P}$ = 37.1 kW, and relative pressure drop ($\Delta p/P$) across nozzle of 3% (see Table 1). The time-averaged OH* chemiluminescence images are normalized by the maximum OH* value in each case to facilitate comparison. During pure Jet-A1 operation, the high-luminosity reaction zone is distributed over a broad area and located far from the fuel nozzle (Fig. 4a). It is evident that the flame is lifted, enabling a certain degree of pre-evaporation and premixing of Jet-A1 fuel with air. At 15% H_2 fuel split, the flame shape closely resembles that of the pure Jet-A1 case, attributed to the low radial H_2 jet penetration (Fig. 4b). However, as the H_2 content increases, the flame becomes more compact and shifts closer to the fuel nozzle due to the higher flame speed and reactivity of H_2-rich fuel, as depicted in Fig. 4(c–e). At 30% H_2 fuel split, the flame is notably closer to the nozzle exit (Fig.

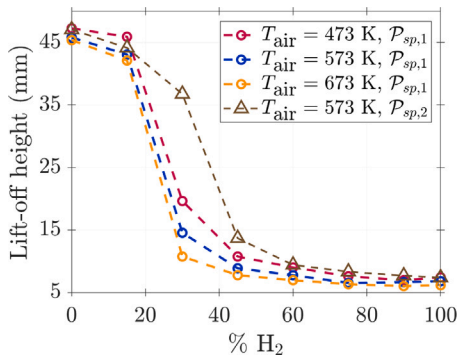

Fig. 6. Effect of H_2 blend on the flame position/lift-off height (LOH) for different T_{air} and $\mathcal{P}_{sp}$. The operating conditions are provided in Table 1.

4c). This behavior reflects that the increased radial H_2 jet penetration leads to an accumulation of H_2 fuel closer to the wall of the fuel nozzle. Thus, the flame can stabilize more near the burner exit with the help of the outer recirculation zone.

As the H_2 content increases to 45%, the reaction region moves further inward, closer to the nozzle exit (Fig. 4d). Additionally, the presence of Jet-A1 leads to higher heat release intensities over a longer distance from the fuel nozzle, allowing the flame to maintain a broader structure. For H_2 content from 45% to 100%, the flame shape near the burner exit remains nearly unchanged, while the flame length consistently decreases as the portion of Jet-A1 decreases (intermediate conditions not shown here for brevity). At 100% H_2, the flame exhibits a highly compact reaction zone, positioned near the burner exit yet remaining distinctly detached from the burner (Fig. 4e).

Fig. 5 shows the time-averaged OH* chemiluminescence flame shapes at T_{air} = 673 K and ϕ values corresponding to the different fuel splits are identical to those shown in Fig. 4(a–e). In typical gas turbine operations, the relative pressure drop remains constant regardless of changes in T_{air}. As a result, higher T_{air} leads to increased bulk velocities (U_b), as shown in Table 1. This effect is balanced by an elevated laminar flame speed at higher temperatures. Additionally, the higher air inlet temperatures influence the degree of pre-evaporation and premixing, potentially resulting in a more homogeneous fuel-air mixture. Overall, these factors combine to yield only a slight reduction in the lift-off height at higher T_{air} (Fig. 5a). A significantly more compact reaction zone can be observed for the pure Jet-A1 case at elevated T_{air}, compared to Fig. 4(a). A further explanation is that the enhanced outer recirculation zone at elevated T_{air} results from the reduced expansion ratio between fresh and burnt gases, as described by Shamma et al. [23] for a lean lifted spray flame.

Importantly, the progressive relocation of the reaction zone toward the fuel nozzle with increasing H_2 content is more pronounced in Fig. 5(b–e) compared to the flame shape observed in Fig. 4(b–e). For instance, at 30% H_2 content, the high-luminosity reaction zone shifts closer to the fuel nozzle exit and becomes compact, compared to Fig. 4(c). In the case of pure H_2 operation, a highly compact reaction zone is observed (Fig. 5e). Although increasing the fuel split beyond 30% degrades premixing quality and produces near-stoichiometric pockets at large radii near the mixing tube exit, the location of the high-luminosity reaction zone remains unchanged. This invariance likely reflects the burner design, which promotes a homogeneous and high-velocity airflow at the burner exit. Additionally, the injection angle of H_2 jets enhances the axial velocity component as H_2 fuel split increases.

4.2. Lift-off height with H_2 content variation

The flame lift-off height is a crucial parameter for characterizing flame stability because it governs the degree of fuel-air mixing before combustion and serves as a key indicator of pollutant emission performance. The lift-off height is defined as the distance from the jet outlet to the flame base. Here, the lift-off height was determined based on high-speed OH* chemiluminescence measurements and defined as the distance from the fuel nozzle exit to the horizontal line upstream of which 5% of the total chemiluminescence intensity is detected. This relatively low threshold was chosen to minimize the impact of different OH* intensities from the Jet-A1 and H_2 flame on the results.

The variation of lift-off height with increasing H_2 content at specific thermal powers $\mathcal{P}_{sp,1}$ = 1.46 MJ/kg$_{air}$ and $\mathcal{P}_{sp,2}$ = 1.02 MJ/kg$_{air}$ is shown in Fig. 6. For $\mathcal{P}_{sp,1}$, as the H_2 concentration increases, the flame lift-off height significantly decreases for different T_{air}. The lift-off height is at first only slightly reduced for up to 15% H_2, which is related to an increased flame speed by H_2 addition in combination with a low radial H_2 jet penetration. For 30% H_2 content, the flame is starting to anchor in the outer recirculation zone near the burner exit. This change is primarily due to the large radial H_2 jet penetration, which leads to a burnable mixture at the outer recirculation zone near the nozzle exit (see Fig. 4c and 5c). For further increasing fuel split, more non-homogeneous H_2 fuel concentration is expected, with the radial H_2 jets potentially impinging the mixing tube wall near the nozzle exit.

The lift-off height at $\mathcal{P}_{sp,2}$ (Fig. 6), corresponds to the operating condition near lean blowout (LBO). For up to 15% H_2 content, the lift-off height remains close to that of the $\mathcal{P}_{sp,1}$ case at T_{air} = 573 K. With H_2 content increased up to 45%, the lift-off height remains higher than at $\mathcal{P}_{sp,1}$, likely due to weaker radial H_2 jet penetration at lower thermal power, which promotes premixing above the burner exit. Beyond 45% H_2, the lift-off height follows a trend similar to that observed at $\mathcal{P}_{sp,1}$, likely resulting from poorer fuel homogeneity, as higher H_2 content leads to stronger radial jets that accumulate near the mixing tube exit at larger radii.

4.3. Lean blowout limits during fuel flexible operation

Investigating the relationship between fuel composition and flame blowout limit is of significant importance in the design of lean combustion burners. Excessively lean combustion can destabilize the flame, leading to blowout caused by phenomena such as local extinction from high strain rates. Understanding and controlling this stability range is vital to ensure safe operation and minimize pollutant emissions. The lean blowout (LBO) limit is defined as the maximum air-to-fuel ratio at which combustion can be sustained before flame extinction or blowout, which determines the minimum fuel flow required for stable operation under specific conditions. In this experiment, the lean blowout limit of Jet-A1/H_2/air flames was measured by maintaining a constant U_b as outlined in Table 1, while gradually reducing ϕ until the flame blowout occurred.

The LBO limits of the low swirling flame at varied H_2 fuel splits for three different T_{air} are shown in Fig. 7. Error bars represent the standard deviation in the estimation of the LBO equivalence ratio (ϕ_{LBO}) across three experimental runs. At T_{air} = 473 K, ϕ_{LBO} decreases significantly from 0.37 (pure Jet-A1) to 0.2 (100% H_2). This reduction becomes more pronounced at higher T_{air}, with ϕ_{LBO} dropping from 0.36 to 0.16 at T_{air} = 573 K and 0.34 to 0.14 at T_{air} = 673 K under the same H_2 fuel split.

A pure Jet-A1 flame exhibits higher ϕ_{LBO} across different T_{air} compared to pure H_2 flames. For H_2 content up to 30%, the influence of H_2 on ϕ_{LBO} remains relatively consistent across different T_{air}. This behavior likely arises from limited H_2 jet penetration and the continued dominance of Jet-A1 in the combustion process. However, for H_2 contents exceeding 30%, an higher reduction in ϕ_{LBO} is observed with increase in H_2 concentrations. This decrease results from the enhanced reaction rate, greater diffusivity, and higher burning velocity for H_2-enriched flames. A clear divergence in LBO limits emerges across different T_{air}. For H_2 contents up to 90%, significantly lower values of ϕ_{LBO} are observed, whereas pure H_2 operation results in slightly

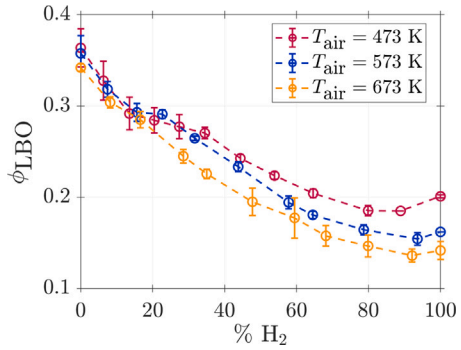

Fig. 7. Effect of H_2 blend on lean blowout (LBO) limits for different T_{air}. Error bars show the standard deviation of ϕ_{LBO} from three runs. The operating conditions are provided in Table 1.

Table 2
Assessment of flashback limits across the investigated operating conditions at T_{air} = 673 K and $\phi = 0.7$.

$\Delta p/P$(%)	$\dot{m}_{air}$(g/s)	$\mathcal{P}$ (kW)	U_b (m/s)	FB
3	21.2	43.6	90.5	No
2	17.3	35.6	73.9	No
1	12.2	25.2	52.2	No

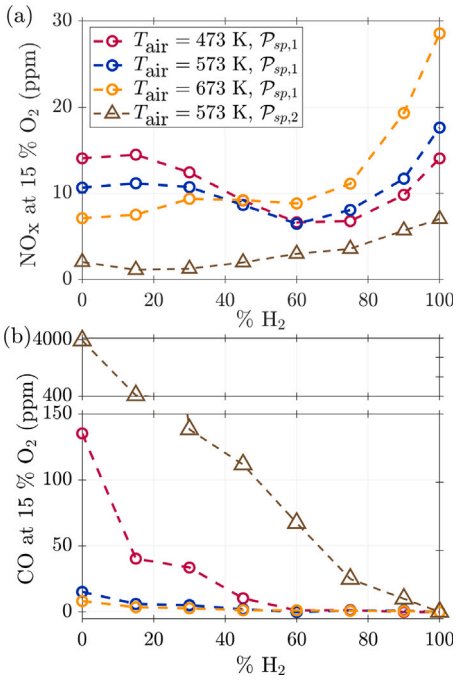

Fig. 8. Variation of NO_x and CO emissions as a function of H_2 blend for different T_{air} and $\mathcal{P}_{sp}$, with operating conditions detailed in Table 1.

higher ϕ_{LBO}. Interestingly, the LBO limit for the pure H_2 case is more restrictive than that of a 90% H_2 fuel split. One plausible explanation is that the residual Jet-A1 in the fuel stream alters the local air-fuel mixture distribution, which helps stabilize the flame compared to the gaseous fuel. Overall, the influence of T_{air} on LBO for pure Jet-A1 is less pronounced than for pure H_2 (Fig. 7). Moreover, switching from Jet-A1 to H_2 through intermediate blends improves flame stability, enabling the lean blowout limit to move towards a lower equivalence ratio and expanding the stabilization regime of the fuel-flexible combustor.

4.4. Flashback limits

A critical issue in H_2 combustion is the risk of fast upstream flame propagation, which can lead to flame stabilization in the mixing tube, where fuel and air mix before entering the combustion chamber, referred to as flashback (FB) [25]. Increased propensity for flashback is influenced by factors such as mixing quality, equivalence ratio, flow velocity, and combustor design. In our combustor, no flame flashback was observed, for ϕ up to 0.7 and reduced air mass flow rates corresponding to $\Delta p/P$ values from 3% to 1% in the pure H_2 experiments (see Table 2). Instantaneous OH^* chemiluminescence images for all operating conditions listed in Table 2 confirmed that the reaction zone remained near the burner exit while staying detached, with no signs of flashback. This indicates that the nominal $\dot{m}_{air}$, $\mathcal{P}$, and U_b at $\phi = 0.7$ (as given in Table 2), can be reduced by at least 58% without causing flashback. This flashback safety margin is extremely promising, since for operating conditions above 30% H_2 at nominal power (as outlined in Table 1), flammable mixtures are expected near the external wall at the nozzle exit.

4.5. NO_x and CO emission characteristics

Fig. 8 shows the concentrations of NO_x ($NO + NO_2$) and CO in ppm (at 15% O_2) for various H_2 contents, at two specific thermal powers ($\mathcal{P}_{sp,1}$ and $\mathcal{P}_{sp,2}$), under conditions detailed in Table 1. The reported NO_x and CO values correspond to the averaged measurements, as fluctuations were minimal (±0.5 ppm NO_x, ±3 ppm CO). Fig. 8(a) illustrated the impact of H_2 blends on the NO_x emissions with an increase in T_{air}. For the nominal power condition $\mathcal{P}_{sp,1}$, the overall NO_x concentration in the pure Jet-A1 case is lower than in the pure H_2 case, as the flame is lifted promotes better premixing. Increasing T_{air} accelerates pre-evaporation and enhances premixing for the Jet-A1 content, which improves fuel–air homogeneity and lowers overall NO_x emissions levels. With H_2 content increased up to 45%, low T_{air} conditions show lower NO_x emission levels whereas high T_{air} condition shows increase in the NO_x emissions. This behavior is due to higher adiabatic flame temperatures. At even higher H_2 contents, the local fuel–air mixture is expected to become richer due to very large radial H_2 jet penetration reaching the nozzle wall, leading to locally high flame temperatures and an increased formation of NO_x emissions. In pure H_2 case, a significant increase in NO_x emissions for higher T_{air} compared to low T_{air} can be explained by the combination of higher adiabatic flame temperatures and poorer mixing.

For $\mathcal{P}_{sp,2}$, corresponding to the operating condition near LBO, NO_x emissions remain below 10 ppm for all fuel splits. NO_x levels are lower for pure Jet-A1 than for pure H_2 due to the lifted flame enhancing premixing. The reduced adiabatic flame temperature and weaker radial H_2 jet penetration keep NO_x emissions low, even at higher H_2 contents, compared to $\mathcal{P}_{sp,1}$.

As anticipated, CO emissions decrease with an increase in H_2 content in the fuel blend (Fig. 8b). For instance at $\mathcal{P}_{sp,1}$, in a mixture without H_2 addition, the maximum of CO emissions reaches 140 ppm at T_{air} = 473 K, 20 ppm at T_{air} = 573 K, and 17 ppm at T_{air} = 673 K. Interestingly, even a modest H_2 fuel split of 15% results in a significant reduction in CO emissions, from 140 ppm to 40 ppm, at low T_{air} of 473 K. CO emission levels become nearly identical for higher H_2 contents beyond 45% across all T_{air}. This operating condition is particularly important for the lowest thrust conditions in aero engines, such as idle and taxiing at airports. For very high H_2 blends, CO emissions approach near-zero levels. In contrast, for $\mathcal{P}_{sp,2}$ which is close to the LBO limit, CO emissions reach 4000 ppm for pure Jet-A1, whereas a fuel split of 15% results in a significant reduction in CO emissions to 400 ppm. For higher H_2 fuel splits, CO emissions decrease significantly but remain relatively high compared to $\mathcal{P}_{sp,1}$.

5. Conclusions

This paper explores the fuel flexibility of a laboratory-scale combustor operating with Jet-A1 and H_2. The lean-lifted flame concept is utilized to stabilize flames with the addition of H_2. Under air preheating temperatures ranging from 473 K to 673 K, increasing the H_2 concentration shifts the flame stabilization closer to the fuel nozzle exit, reducing the lift-off height. Additionally, dual-fuel operation significantly extends the LBO limits. While lower H_2 blends result in minimal changes to LBO limits, higher blends of H_2 improve the LBO limits by nearly a factor of two.

The investigated combustor configuration remains flashback safe for an equivalence ratio up to 0.7 and down to 58% of the nominal air mass flow of 21.2 g/s, at an air preheating temperature of 673 K. The combustor also remains flashback safe even with up to 100% H_2, despite the radial H_2 jet penetration not being optimal beyond a fuel split of 30%.

Finally, at higher specific thermal power, NO_x emissions decrease at low and increase at high air inlet temperatures for H_2 fuel splits up to 45%. For fuel splits between 45% and 75% H_2, emissions remain roughly around 10 ppm, rising significantly only at higher blends. In contrast, at lower specific thermal power near LBO, NO_x emissions remain below 10 ppm for all fuel splits. This suggests that, despite offering fuel flexibility and very promising overall pollutant emissions performance, the current configuration at higher specific thermal power is not optimal for H_2 fuel splits above a certain threshold. Therefore, for higher H_2 fuel splits, incorporating additional stageable H_2 injection holes will further reduce NO_x emissions and improve flashback margins. Additionally, even a small H_2 fuel split of 15% results in a significant reduction in CO emissions for low air inlet temperature, which is important for low thrust conditions for aero engines.

CRediT authorship contribution statement

Samarjeet Singh: Writing – review & editing, Writing – original draft, Methodology, Investigation, Formal analysis, Conceptualization. **Matteo Amerighi:** Writing – review & editing, Formal analysis. **Nicola Scopolini:** Writing – review & editing, Formal analysis. **Antonio Andreini:** Writing – review & editing, Supervision. **Stefan R. Harth:** Writing – review & editing, Formal analysis, Conceptualization. **Dimosthenis Trimis:** Writing–review & editing, Supervision.

Novelty and significance statement

The novelty of this research lies in an innovative fuel-flexible burner that combines H_2 injectors in a jet-in-crossflow arrangement with a lean-lifted spray Jet-A1 flame. The experimental results confirm that the combustor delivers flashback-resilient performance under atmospheric conditions across the full range of operation, spanning from pure Jet-A1 to pure H_2. The specific significance of the current study is as follows:

- Lean blowout limits are extended by a factor of two when switching from pure Jet-A1 to pure H_2 operation.
- For up to 75% H_2 fuel split, NO_x emissions are around 10 ppm, which is reduced compared to the already good emissions performance of the lean-lifted spray flame.
- The H_2 injection system is designed for the optimized mixing up to 30% H_2 fuel split; by incorporating additional injection ports, there is significant potential to achieve even greater NO_x reductions.

Declaration of competing interest

The authors declare that they have no known competing financial interests or personal relationships that could have appeared to influence the work reported in this paper.

Acknowledgments

Funded by the European Union

The research leading to these results has received funding from the European Union (Project: FFLECS; Grant agreement ID: 101096436). Views and opinions expressed are however those of the authors only and do not necessarily reflect those of the European Union. Neither the European Union nor the granting authority can be held responsible for them.

References

[1] A. Gomez, H. Smith, Liquid hydrogen fuel tanks for commercial aviation: Structural sizing and stress analysis, Aerosp. Sci. Technol. 95 (2019) 105438.
[2] A. Baroutaji, T. Wilberforce, M. Ramadan, A.G. Olabi, Comprehensive investigation on hydrogen and fuel cell technology in the aviation and aerospace sectors, Renew. Sustain. Energy Rev. 106 (2019) 31–40.
[3] E.-A. Tingas, A.M. Taylor, Hydrogen: Where it can be used, how much is needed, what it may cost, in: Hydrogen for Future Thermal Engines, Springer, 2023, pp. 3–64.
[4] E.J. Adler, J.R. Martins, Hydrogen-powered aircraft: Fundamental concepts, key technologies, and environmental impacts, Prog. Aerosp. Sci. 141 (2023) 100922.
[5] S. Manigandan, T. Praveenkumar, J.I. Ryu, T.N. Verma, A. Pugazhendhi, Role of hydrogen on aviation sector: A review on hydrogen storage, fuel flexibility, flame stability, and emissions reduction on gas turbines engines, Fuel 352 (2023) 129064.
[6] T. Sattelmayer, C. Mayer, J. Sangl, Interaction of flame flashback mechanisms in premixed hydrogen–air swirl flames, J. Eng. Gas Turbine. Power 138 (1) (2016) 011503.
[7] H.H.-W. Funke, N. Beckmann, J. Keinz, A. Horikawa, 30 years of dry-low-NO_x micromix combustor research for hydrogen-rich fuels—An overview of past and present activities, J. Eng. Gas Turbine. Power 143 (7) (2021) 071002.
[8] S.R. Hernandez, Q. Wang, V. McDonell, A. Mansour, E. Steinthorsson, B. Hollon, Micro mixing fuel injectors for low emissions hydrogen combustion, in: Turbo Expo: Power for Land, Sea, and Air, vol. 43130, 2008, pp. 675–685.
[9] W. Bilger, R. Dibble, Differential molecular diffusion effects in turbulent mixing, Combust. Sci. Technol. 28 (3–4) (1982) 161–172.
[10] M. Chen, L. Zhang, C. Xing, Y. Bao, P. Qiu, W. Zhang, S. Sun, Y. Zhao, Experimental and numerical simulation study of the effect of mixing on the characteristics of swirl/non-swirl micromix flames, Energy 307 (2024) 132570.
[11] B. Kruljevic, N. Darabiha, D. Durox, N. Vaysse, A. Renaud, R. Vicquelin, B. Fiorina, Experimentation and simulation of a swirled burner featuring cross-flow hydrogen injection with a focus on the OH* chemiluminescence, Combust. Flame 273 (2025) 113945.
[12] S. Burmberger, T. Sattelmayer, Optimization of the aerodynamic flame stabilization for fuel flexible gas turbine premix burners, J. Eng. Gas Turbine. Power 133 (10) (2011) 101501.
[13] T.G. Reichel, S. Terhaar, O. Paschereit, Increasing flashback resistance in lean premixed swirl-stabilized hydrogen combustion by axial air injection, J. Eng. Gas Turbine. Power 137 (7) (2015) 071503.
[14] H. Hiroyasu, M. Arai, T. Kadota, J. Yoso, An experimental study on kerosene-hydrogen hybrid combustion in a gas turbine combustor, Bull. JSME 23 (184) (1980) 1655–1662.
[15] G. Juste, Hydrogen injection as additional fuel in gas turbine combustor. evaluation of effects, Int. J. Hydrog. Energy 31 (14) (2006) 2112–2121.
[16] J. Frenillot, G. Cabot, M. Cazalens, B. Renou, M. Boukhalfa, Impact of H_2 addition on flame stability and pollutant emissions for an atmospheric kerosene/air swirled flame of laboratory scaled gas turbine, Int. J. Hydrog. Energy 34 (9) (2009) 3930–3944.
[17] J. Burguburu, G. Cabot, B. Renou, A.M. Boukhalfa, M. Cazalens, Effects of H_2 enrichment on flame stability and pollutant emissions for a kerosene/air swirled flame with an aeronautical fuel injector, Proc. Combust. Inst. 33 (2) (2011) 2927–2935.
[18] L. Miniero, K. Pandey, G. De Falco, A. D'Anna, N. Noiray, Soot-free and low-NO combustion of jet A-1 in a lean azimuthal flame (LEAF) combustor with hydrogen injection, Proc. Combust. Inst. 39 (4) (2023) 4309–4318.
[19] K. Dave, S. Link, F. De Domenico, F. Schrijer, F. Scarano, A.G. Rao, Kerosene-H_2 blending effects on flame properties in a multi-fuel combustor, Fuel Comms. (2025) 100139.
[20] H.A. Alabaş, B.A. Çeper, Effect of the hydrogen/kerosene blend on the combustion characteristics and pollutant emissions in a mini jet engine under CDC conditions, Int. J. Hydrog. Energy 52 (2024) 1275–1287.
[21] P. Fu, Y. Wang, L. Hou, Numerical study on combustion of a novel micromix multi-nozzles for kerosene/hydrogen fuels, in: Turbo Expo: Power for Land, Sea, and Air, vol. 87943, American Society of Mechanical Engineers, 2024, V03AT04A064.

[22] L. Palanti, L. Mazzei, C. Bianchini, S. Link, K. Dave, F. de Domenico, A.G. Rao, CFD-based scouting for the design of a multi-fuel kerosene/hydrogen atmospheric burner, in: 34th ICAS Congress, ICAS, 2024, pp. ICAS–2024.
[23] M. Shamma, S. Harth, D. Trimis, Experimental investigation of multi-burner array with lean lifted spray flames in inline and inclined configurations, Appl. Energy Combust. Sci. 17 (2024) 100246.
[24] N. Kerr, D. Fraser, Swirl part 1: Effect on axisymmetrical turbulent jets, J. Inst. Fuel 38 (299) (1965) 519.
[25] Z. Shi, H. Xu, L. Cui, Y. Dong, Burner, combustion characteristic and flame stabilization mechanism in micromix combustion: A review, Renew. Sust. Energy Rev. 225 (2026) 116164.